Supporting Information

Metal–organic rotaxane frameworks constructed by cucurbit[8]uril-based ternary complex for selective detection of antibiotics

Weijie Wu, Yinghao Xu, Shoujun Wang, Qingqing Pang*, Simin Liu*

Key Laboratory of Hubei Province for Coal Conversion and New Carbon Materials, School of Chemistry and Chemical Engineering, Wuhan University of Science and Technology, Wuhan 430081, China

* Corresponding authors.

E-mail addresses: pangqingqing@wust.edu.cn (Q. Pang), liusimin@wust.edu.cn (S. Liu)

Table of contents page

1. Chemicals and Methods

All chemicals were purchased from commercial suppliers and used without further purifications. Solution ^{1}H nuclear magnetic resonance (^{1}H NMR) spectra were obtained on Agilent 600 MHz DD2 Spectrometer. Powder X-ray diffraction (PXRD) patterns were obtained from a Rigaku Smart Lab SE X-ray powder diffractometer at 3 kW power (50 kV, 60 mA) with Cu *K*α radiation. The simulated PXRD patterns were calculated by the single-crystal structural data on Mercury 3.10.3. Fourier transform infrared spectroscopy (FT-IR) measurements were carried out on a INVENIO R FT-IR spectrometer with KBr pellets. Thermogravimetric analyses (TGA) of the activated samples were conducted on a TA-Q500 instrument under N_2 atmosphere with a heating rate of 10 °C·min^{-1}. Elemental analyses were performed by using a vario EL element analyzer. Fluorescence spectra were obtained on a PerkinElmer LS-55 instrument. Ultraviolet–visible (UV-Vis) spectroscopy measurements were performed on a SHIMADZU UV-3600 instrument. Single crystal X-ray diffraction (SXRD) data were collected on a Bruker Apex III single crystal X-ray diffractometer equipped with photon II detector and operated at 70 kV, 3.57 mA to generate Ga *K*α radiation (λ = 1.34138 Å).

2. Chemical Synthesis

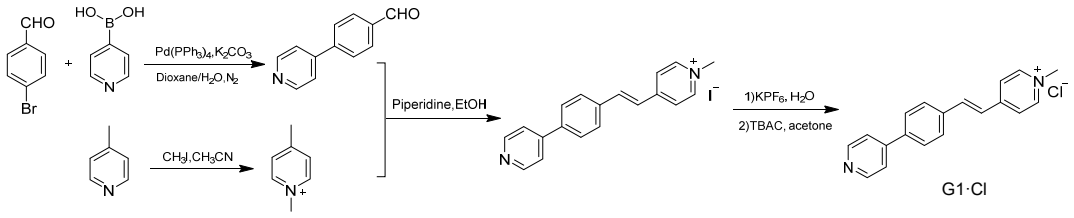

Fig. S1 The synthetic procedures of G1·Cl.

2.1 Synthesis of 4-(4-Pyridyl)benzaldehyde

Under the nitrogen atmosphere, a mixture of 4-bromobenzaldehyde (1.4 g, 7.56 mmol), 4-pyridineboronic acid (1.1 g, 8.95 mmol), $Pd(PPh_3)_4$ (250 mg, 0.22 mmol) and K_2CO_3 (2.07 g, 19.6 mmol) in dioxane/H_2O (4 : 1, 50 mL) was heated at 80 °C for 48 h. After cooling to room temperature, deionized water (120 mL) was poured into the reaction mixture and the aqueous phase was extracted with DCM. The crude product was purified by flash silica gel column chromatography (PE : EA = 2:1 in volume).

2.2 Synthesis of 1,4-Dimethylpyridinium Iodide

Methyl iodide was added to the solution of 4-methylpyridine in CH_3CN at room temperature. The white precipitate was produced immediately in an exothermic reaction. The solid was filtered and washed with CH_3CN.

2.3 Synthesis of (*E*)-1-Methyl-4-(4-(pyridin-4-yl)styryl)pyridinium (G1) Chlorine

The synthesis of (*E*)-1-methyl-4-(4-(pyridin-4-yl)styryl)pyridinium iodide was conducted according to a reported procedure with slight modification.[1] There are two

steps to ion exchange: First, iodide of G1 (800 mg, 2.00 mmol) was added to the aqueous solution (30 mL) of KPF_6 (920 mg, 4.02 mmol) under stirring for 1 h. The purple precipitate was collected by centrifugation and washed twice with deionized water. Hexafluorophosphate of G1 was obtained after dried at 80 ºC overnight. Next, hexafluorophosphate of G1 was added to the acetone solution (20 mL) of tetrabutyl ammonium chloride (TBAC, 1.10 mg, 3.95 mmol) under stirring for 2 h. The dark purple precipitate was collected via centrifugation and washed with acetone 2-3 times. The chlorine product was dried at 60 ºC overnight. ^{1}H NMR (600 MHz, D_2O) δ 8.57 (d, J = 5.4 Hz, 2H), δ 8.53 (d, J = 6.4 Hz, 2H), δ 7.99 (d, J = 6.4 Hz, 2H), δ 7.85 (d, J = 8.1 Hz, 2H), δ 7.80 (d, J = 8.1 Hz, 2H), δ 7.75 (d, J = 5.7 Hz, 2H), δ 7.72 (d, J = 16.4 Hz, 1H), δ 7.30 (d, J = 16.3 Hz, 1H), δ 4.25 (s, 3H).

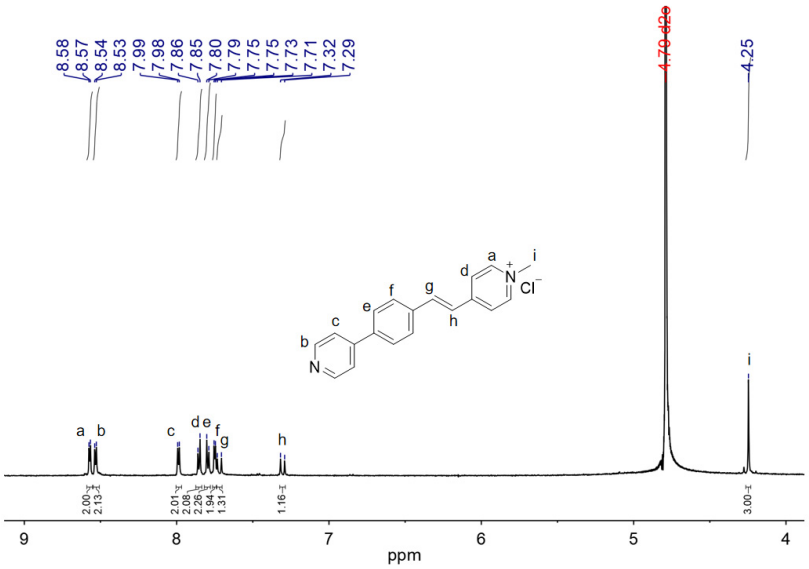

Fig. S2 ^{1}H NMR spectrum of G1 in D_2O (298 K).

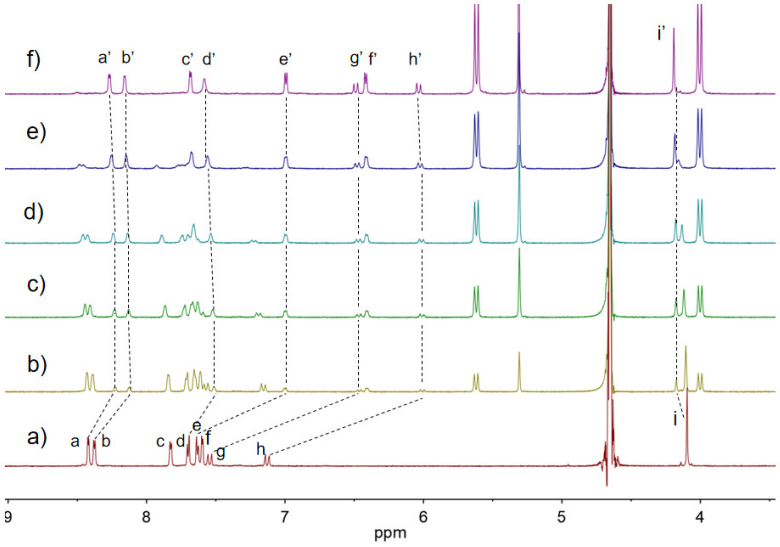

Fig. S3 ^{1}H NMR spectra (600 MHz, 298K, D_2O) of a) free G1 (2 mM); b) with 0.1 eq. of CB[8]; c) with 0.2 eq. of CB[8]; d) with 0.3 eq. of CB[8]; e) with 0.4 eq. of CB[8]; and f) with 0.5 eq. of CB[8].

2.4 Synthesis of WUST-1

$Zn(NO_3)\cdot 6H_2O$ (24.0 mg, 0.08 mmol) and *m*-H_2BDC (6.8 mg, 0.04 mmol) were dissolved in 0.5 mL DMF, then added into the aqueous solution (2 mL) of G1 chlorine (6.1 mg, 0.02 mmol) and CB[8] (13.2 mg, 0.01 mmol). The mixture was heated at 110 ℃ for 48 h in a teflon-lined stainless-steel autoclave. Yellow square crystals were obtained after cooling down to room temperature. Yield: 17 % based on CB[8]. Elemental analysis for activated WUST-1: Calc. (Found, %) for [Zn(*m*-BDC)(G1)$(CB[8])_{0.5}$(HCOO)] ($ZnC_{52}O_{14}N_{18}H_{46}$) C = 51.52 (47.51); H = 3.79 (4.14); N = 20.80 (23.19). FT-IR: (KBr, 4000–500 cm^{-1}): 3414(vs), 2923(w), 2857(w), 2366(w), 2342(w), 1723(s), 1606(s), 1470(s), 1380(s), 1308(w), 1233(s), 1190(w), 1124(w), 1034(w), 968(w), 807(s), 751(w), 708(w), 661(w).

2.5 Synthesis of WUST-2：

$CdCl_2\cdot 3H_2O$ (17.6 mg, 0.08 mmol) and H_2DOBDC (8.1 mg, 0.041 mmol) were dissolved in 0.5 mL DMF, then added into the aqueous solution (2 mL) of G1 chlorine (6.1 mg, 0.02 mmol) and CB[8] (13.2 mg, 0.01 mmol). The mixture was heated at 110 ℃ for 48 h in a teflon-lined stainless-steel autoclave. Yellow square crystals were obtained after cooling down to room temperature. Yield: 18 % based on CB[8]. Elemental analysis for activated WUST-2: Calc. (Found, %) for [Cd(DOBDC)(G1)$(CB[8])_{0.5}$(OH)] ($CdC_{51}O_{15}N_{18}H_{46}$) C = 48.80 (43.54); H = 3.58 (4.13); N = 20.09 (21.26). FT-IR: (KBr, 4000–450 cm^{-1}): 3424(s), 2928(w), 2371(w), 2342(w), 1723(s), 1625(s), 1510(w), 1464(s), 1440(w),1370(s), 1312(s), 1224(s), 1190(s), 963(s), 869(w), 812(s), 751(w), 675(w), 535(w).

3. Single Crystal Structure Determinations

The crystal structures of WUST-1 and WUST-2 were solved by direct methods and refined on F^2 by full-matrix least-squares using the Shelxtl-2018 program systems[2] contained on Olex2.[3]

For both WUST-1 and WUST-2, the solvent water molecules in the structures were modelled by using solvent mask. In WUST-1, the atoms (O5, C52, and O14) of the coordinated $HCOO^-$ ligand, and some atoms (C7 and C8) of the styryl moiety of G1 were involved in disorder. PART restraints were used for these atoms. For WUST-2, one B level alert “PLAT420_ALERT_2_B D-H Bond Without Acceptor O16--H16” still exists in the CheckCIF report. This can be explained by the fact that the solvent water molecules in the structure have been modelled by using solvent mask. Thus, there is no suitable acceptor in the structure for the coordinated hydroxyl ($O16-H16^-$) group on Cd1.

The details of crystal data and structure refinements are summarized in Table S1 and S2.

Table S1. Crystal data and structure refinement for WUST-1.

Identification code	WUST-1	
Empirical formula	C52 H70 N18 O26 Zn	
Formula weight	1428.63	
Temperature	293(2) K	
Wavelength	1.34138 Å	
Crystal system	Monoclinic	
Space group	$P2_1/c$	
Unit cell dimensions	a = 15.936(3) Å	α = 90.00º
	b = 18.3877(14) Å	β = 104.97(10)º
	c = 21.801(3) Å	γ = 90.00º
Volume	6171.4(13) $Å^3$	
Z	4	
Density (calculated)	1.538 g/cm^3	
Absorption coefficient	0.921 mm^{-1}	
F(000)	2984	
Crystal size	0.22 x 0.18 x 0.16 mm^3	
Theta range for data collection	2.497 to 53.118º	
Index ranges	-18<=h<=18	
	-21<=k<=21	
	-24<=l<=26	
Reflections collected	48025	
Independent reflections	10835 [R(int) = 0.0385]	
Completeness to theta = 53.118º	99.1%	
Absorption correction	Multi-scan	
Refinement method	Full-matrix least-squares on F^2	
Data / restraints / parameters	10835 / 99 / 813	
Goodness-of-fit on F^2	1.076	
Final R indices [I>2sigma(I)]	R1 = 0.0609, wR2 = 0.1819	
R indices (all data)	R1 = 0.0715, wR2 = 0.1899	
Largest diff. peak and hole	1.846 and -0.885 $e.Å^{-3}$	

Table S2. Crystal data and structure refinement for WUST-2.

Identification code	WUST-2	
Empirical formula	C51 H90 N18 O37 Cd	
Formula weight	1659.80	
Temperature	100(2) K	
Wavelength	1.34138 Å	
Crystal system	Triclinic	
Space group	*P*-1	
Unit cell dimensions	a = 15.0854(5) Å	α = 77.578(2)°
	b = 15.8414(6) Å	β = 73.354(2)°
	c = 16.6026(6) Å	γ = 78.418(10)°
Volume	3671.0(2) $Å^3$	
Z	2	
Density (calculated)	1.502 g/cm^3	
Absorption coefficient	2.178 mm^{-1}	
F(000)	1732	
Crystal size	0.26 x 0.20 x 0.18 mm^3	
Theta range for data collection	2.451 to 57.141°	
Index ranges	-18<=h<=18	
	-19<=k<=19	
	-20<=l<=20	
Reflections collected	67922	
Independent reflections	15015 [R(int) = 0.0525]	
Completeness to theta = 57.141°	99.4%	
Absorption correction	None	
Refinement method	Full-matrix least-squares on F^2	
Data / restraints / parameters	15015 / 1 / 789	
Goodness-of-fit on F^2	1.060	
Final R indices [I>2sigma(I)]	R1 = 0.0507, wR2 = 0.1622	
R indices (all data)	R1 = 0.0611, wR2 = 0.1676	
Largest diff. peak and hole	1.069 and -1.034 $e.Å^{-3}$	

4. Intermolecular Interactions in MORFs

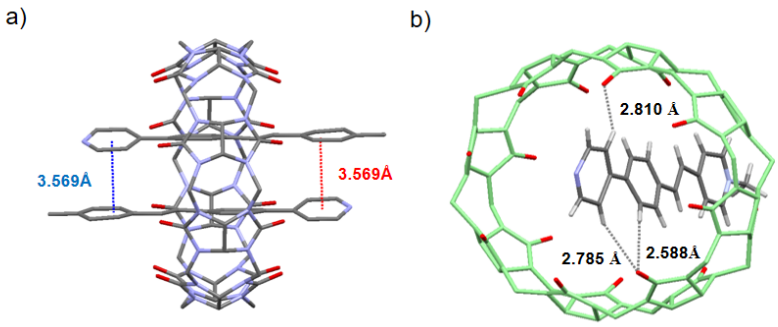

Fig. S4 a) π–π stacking interactions between two encapsulated G1 molecules in the cavity of CB[8] in WUST-1; b) Hydrogen bonding interactions between CB[8] and the encapsulated G1 molecule in WUST-1.

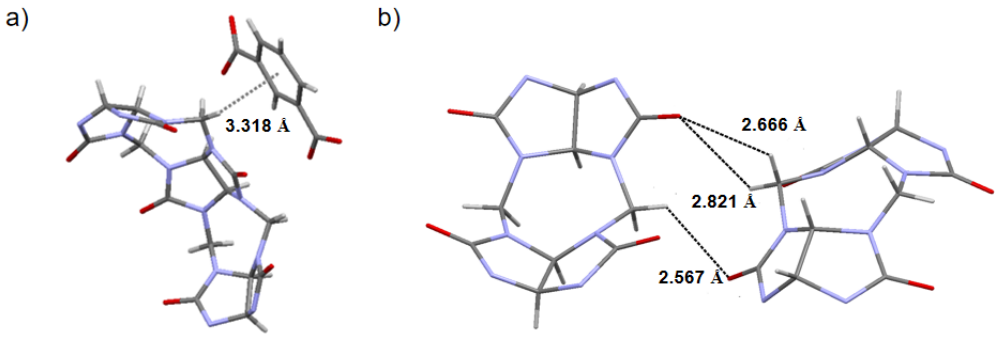

Fig. S5 a) C–H···π interaction between CB[8] and the *m*-BDC linker from two adjacent layers in WUST-1; b) Hydrogen bonding interactions between two CB[8] macrocycles from two adjacent layers in WUST-1.

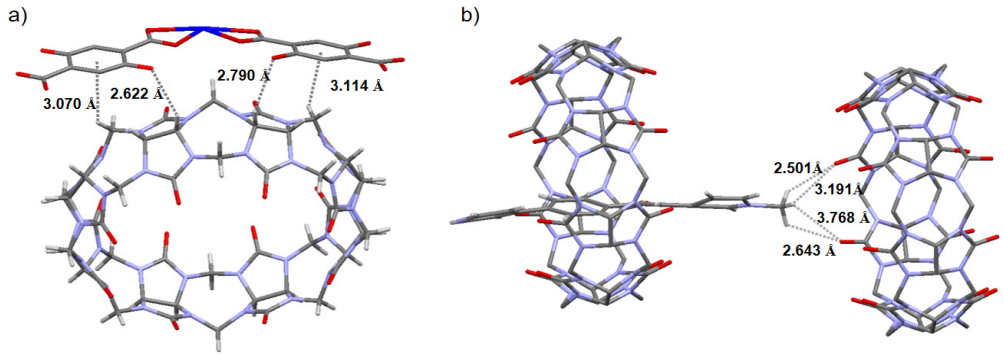

Fig. S6 a) Multiple non-covalent interactions between CB[8] and the DOBDC linker from two adjacent layers in WUST-2; b) Hydrogen bonding interactions between the methyl group of G1 and the portal carbonyls of CB[8] from two adjacent layers in WUST-2.

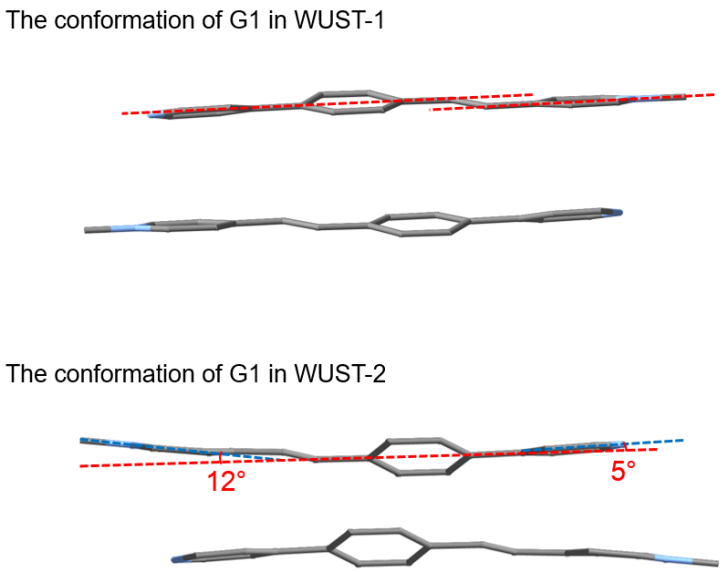

Fig. S7 The conformation of G1 ligand in WUST-1 and WUST-2, respectively.

5. Characterization Data

5.1 FT-IR Spectra of MORFs

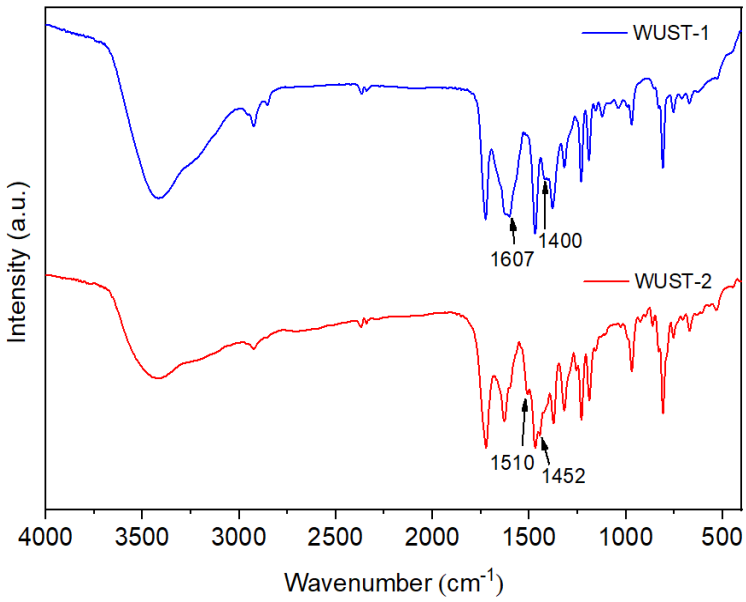

Fig. S8 FT-IR spectra of WUST-1 and WUST-2.

5.2 PXRD Patterns of MORFs

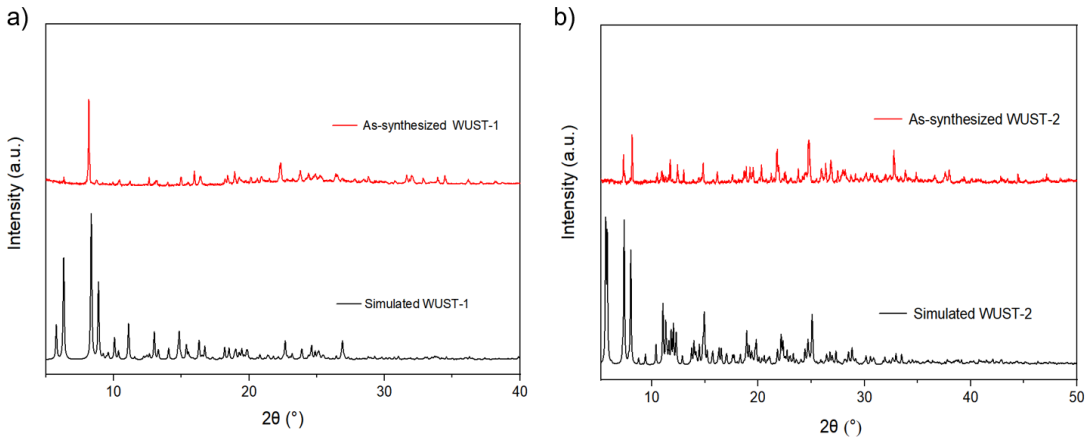

Fig. S9 Simulated and experimental PXRD patterns of a) WUST-1 and b) WUST-2.

5.3 TGA Curves of MORFs

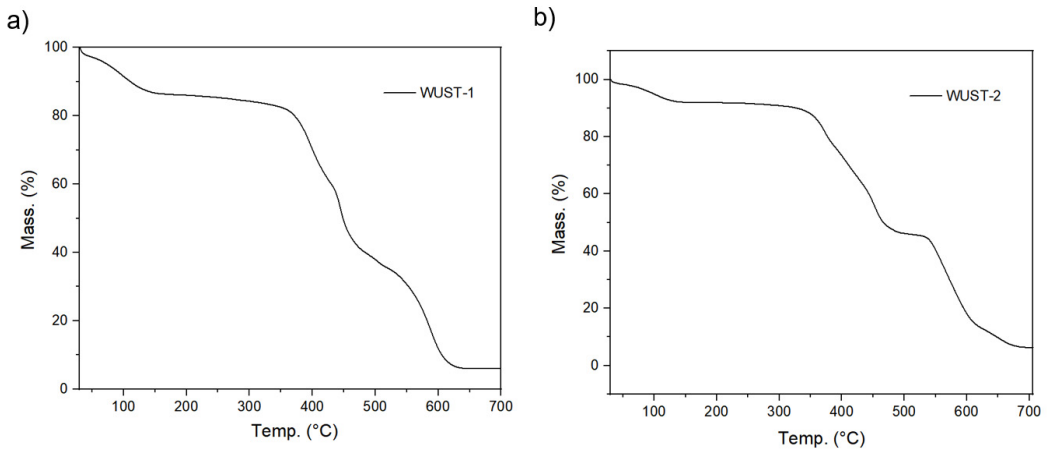

Fig. S10 TGA curve of a) WUST-1 and b) WUST-2.

5.4 PXRD Patterns of MORFs at Different Temperatures

The crystals of WUST-1/WUST-2 (50.0 mg) were placed in a muffle furnace and calcined at different temperatures (100 ℃, 200 ℃, 300℃, and 400℃) under air atmosphere. The samples were calcined at each temperature for 2 hours, and then allowed to cool down to room temperature.

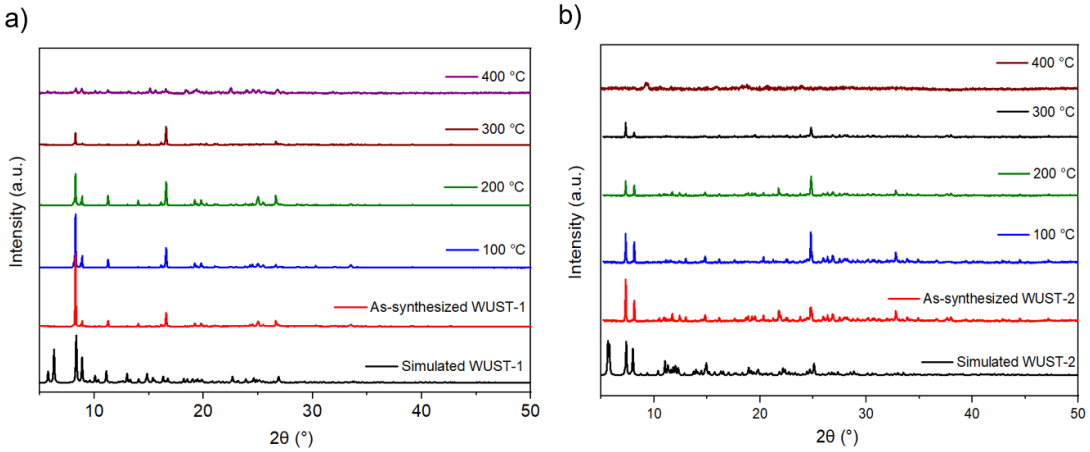

Fig. S11 PXRD patterns of a) WUST-1 and b) WUST-2 calcined at different temperatures.

6. Water Stability Tests

The crystals of WUST-1/WUST-2 (80.0 mg) were soaked in 20 mL deionized water and allowed to stand at room temperature. Partial of the samples were taken every 24 hours and then dried at 60 ℃ for 6 hours in vacuum.

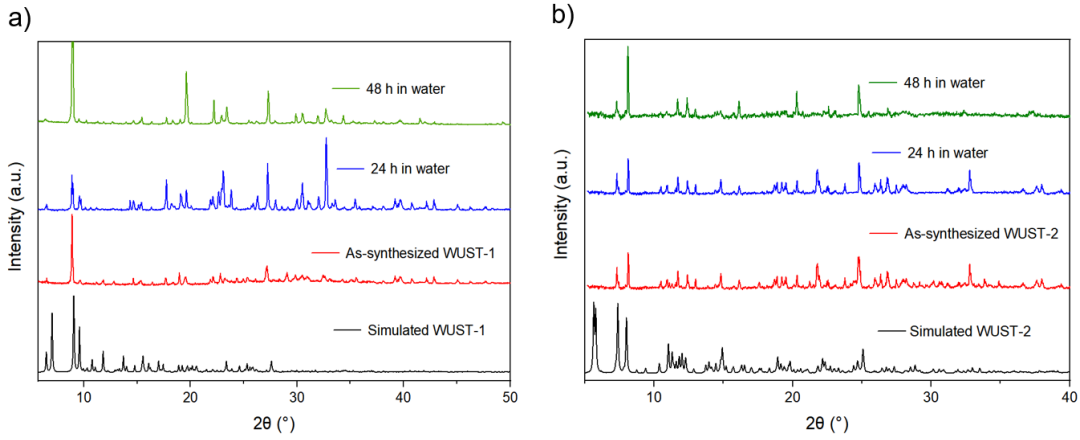

Fig. S12 PXRD patterns of a) WUST-1 and b) WUST-2 in deionized water for different time intervals.

7. Leaking Tests of MORFs in Water

The crystals of WUST-1/WUST-2 (80.0 mg) were soaked in 20 mL deionized water at room temperature. For UV-Vis test, 1 mL supernatant of the samples was taken after soaking MORFs for different time intervals. The concentration of the leaking components was calculated according to the standard curve of CB[8]·$G1_2$ complex (and G1 ligand for WUST-1). The decomposition percentages of WUST-1 and WUST-2 are 3.3% and 1.1%, respectively.

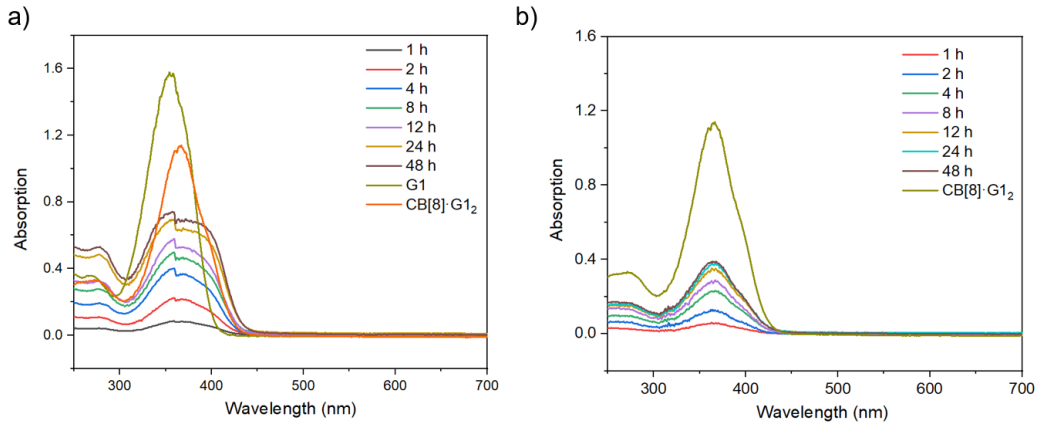

Fig. S13 a) UV-Vis spectra of the free components in water at different time intervals. a) WUST-1 and b) WUST-2.

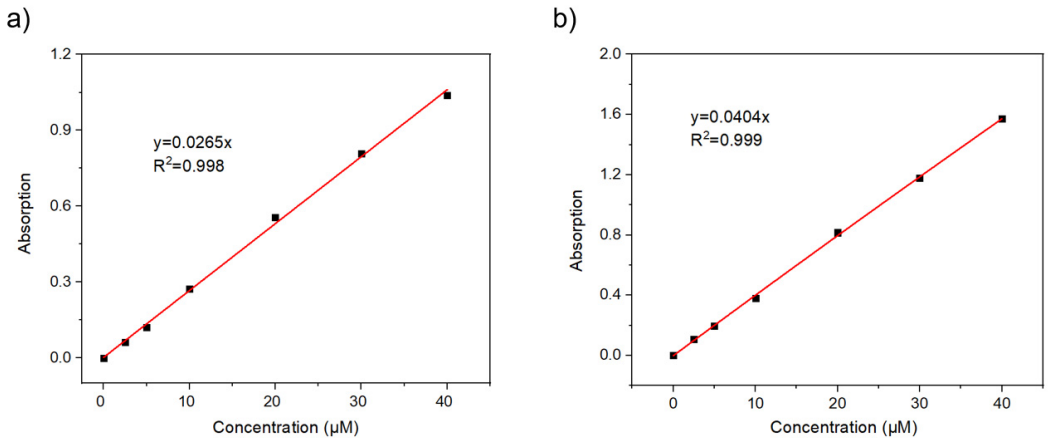

Fig. S14 The linear relationship between a) [CB[8]·$G1_2$] and absorbance, and b) [G1] and absorbance.

8. Detection of Antibiotics

The samples for fluorescence spectroscopy test in aqueous solution were prepared as following. The crystals of WUST-1/WUST-2 (20.0 mg) were dispersed in 10 mL deionized water at room temperature, and then ultrasonically dispersed for 2 minutes to form the uniform suspensions. The powders of G1 for solid-state fluorescence spectroscopy were prepared by freeze-drying of the corresponding aqueous solution.

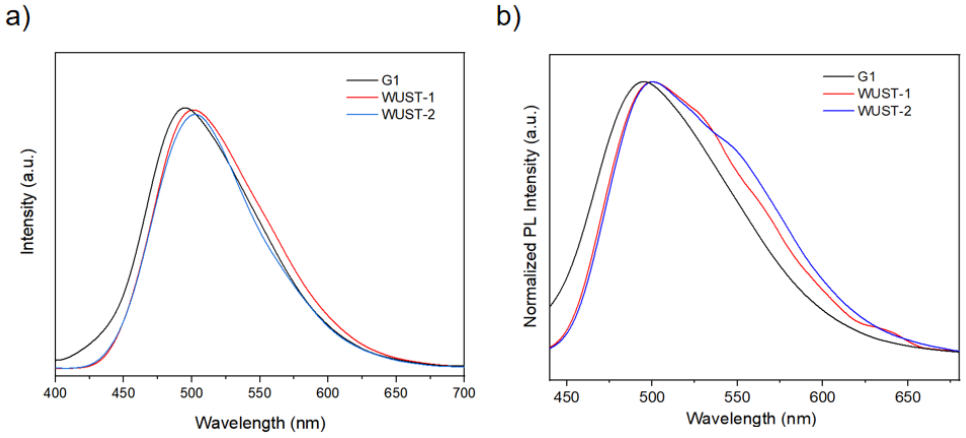

Fig. S15 a) Fluorescence spectra of G1 (0.5 mM), WUST-1 and WUST-2 in aqueous solution, respectively (λ_{ex} = 365 nm); b) Solid-state fluorescence spectra of G1, WUST-1 and WUST-2, respectively (λ_{ex} = 365 nm).

The samples for the detection of antibiotics were prepared by adding 1.0 mL antibiotic solutions with increasing concentrations to the MORF suspensions (1.0 mL). The fluorescence spectra of the suspensions were recorded on the fluorophotometer.

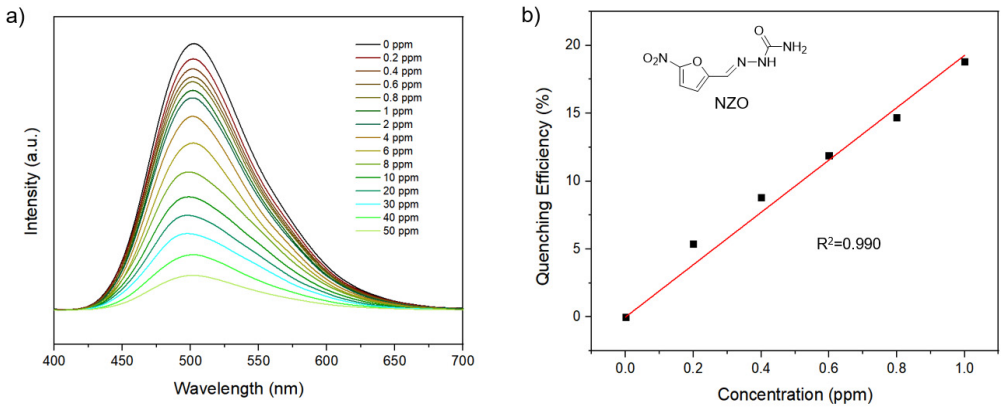

Fig. S16 a) Fluorescence spectra of WUST-1 in water suspension with the addition of different concentrations of NZO (λ_{ex} = 365 nm); b) Correlation between the quenching efficiency and concentration of NZO by WUST-1 (0–1 ppm).

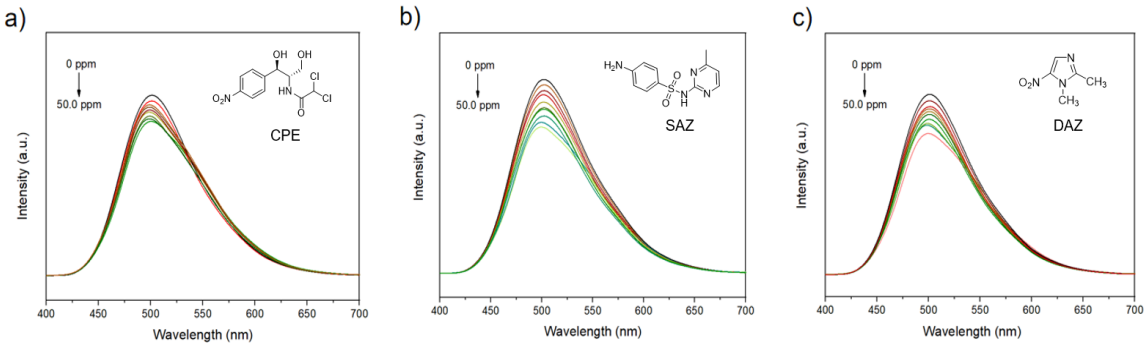

Fig. S17 Fluorescence spectra of WUST-1 in water suspension with the addition of different concentrations of a) CPE; b) SAZ; c) DAZ (λ_{ex} = 365 nm).

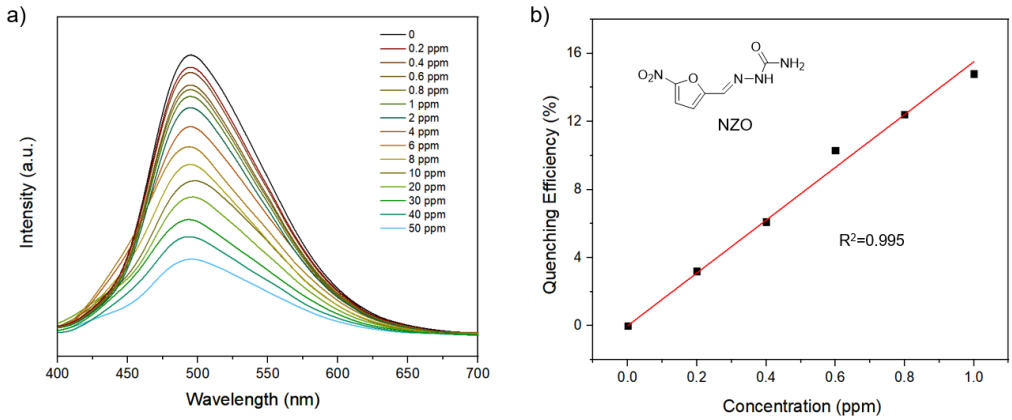

Fig. S18 a) Fluorescence spectra of WUST-2 in water suspension with the addition of different concentrations of NZO (λ_{ex} = 365 nm); b) Correlation between the quenching efficiency and concentration of NZO by WUST-2 (0−1 ppm).

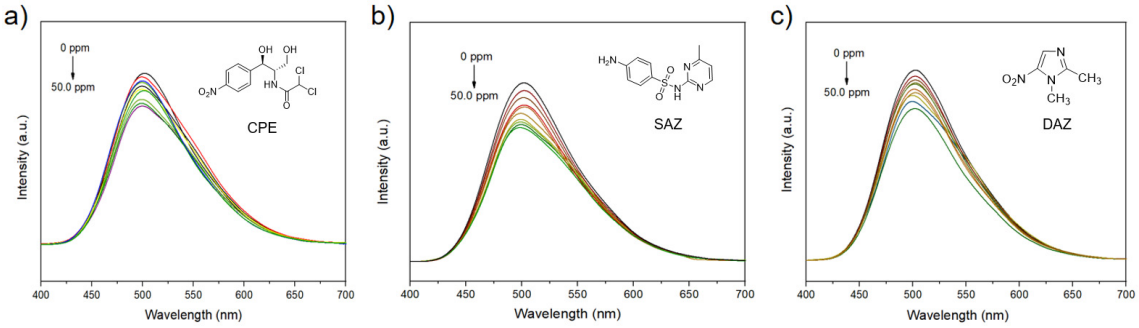

Fig. S19 Fluorescence spectra of WUST-2 in water suspension with the addition of different concentrations of a) CPE; b) SAZ; c) DAZ (λ_{ex} = 365 nm).

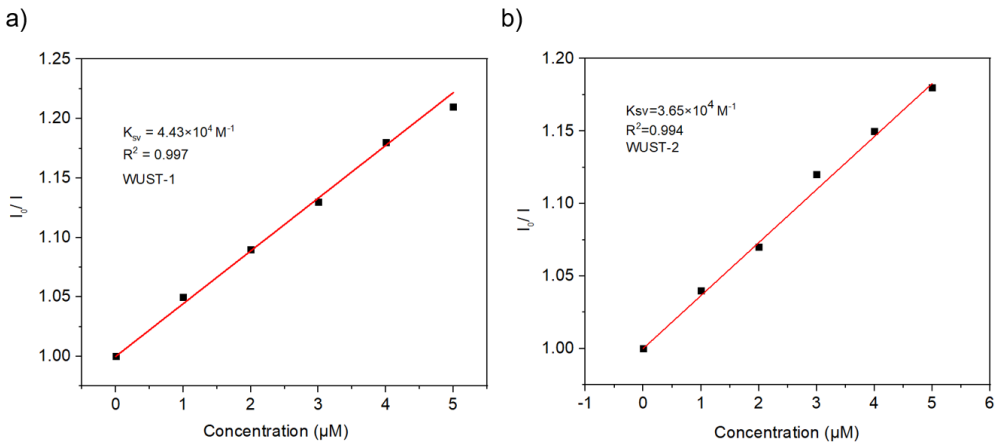

Fig. S20 Stern–Volmer linear relationship between [NZO] and I_0/I for a) WUST-1 and b) WUST-2.

Table S3. The comparison of sensing properties towards NZO of MOFs.

Complexes	Quenching Constant (K_{SV}/M^{-1}) for NZO	LOD (ppm) for NZO	Ref.
WUST-1	4.43×10^4	0.21	This Work
WUST-2	3.65×10^4	0.24	
$[ZnMg(1,4\text{-}NDC)_2(DMF)_2]$ $[Zn_3(\mu_3\text{-}OH)]$	1×10^4	0.79	4
$[Zn(L)]\cdot CH_3CN$	2.41×10^6	0.62	5
$[Zn_4(OH)_2(cbbi)_2(bpee)(H_2O)_4]\cdot 2H_2O$	3.74×10^4	0.22	6
$(Me_2NH_2)_{1.5}[In_{1.5}(FBDC)(BDC)]\cdot 2.5DMF\cdot CH_3CN$	1.83×10^4	0.37	7
$Cd(\mu_3\text{-}HL)_2(H_2O)]\cdot 2.3H_2O$	5×10^6	0.24	8
$Zn(H_2L)(H_2O)_2$	2.41×10^3	1.12	9
$[Zn(L)(phen)]\cdot 0.5DMF$	1.45×10^4	1.07	10
$[Zn_2(L)_2(4,4'\text{-}bipy)]\cdot 4DMF$	1.14×10^4	0.49	
$[Zn_2(Py_2TTz)_2(BDC)_2]\cdot 2(DMF)\cdot 0.5H_2O$	1.72×10^4	0.18	11
$Cd_2(Py_2TTz)_2(BDC)_2]\cdot 2DMF$	4.54×10^4	0.17	

9. Stability Tests of CB[8]·$G1_2$ With Antibiotics

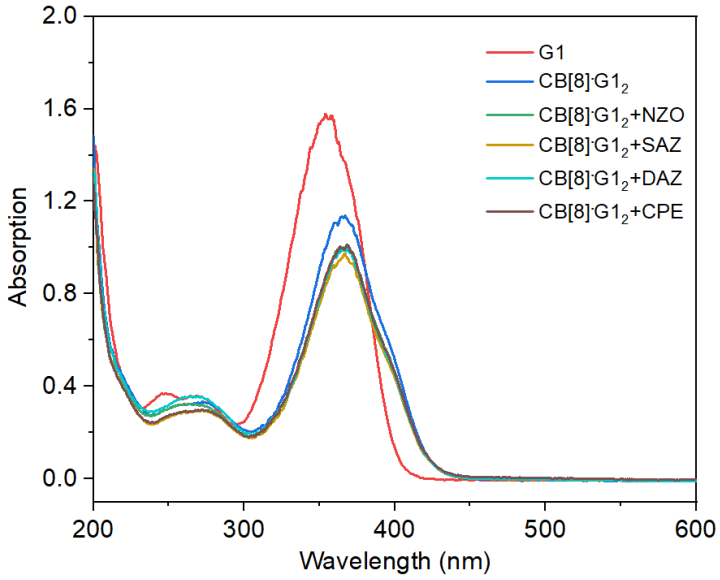

Fig. S21 UV-vis spectra of G1 (40 μM) and CB[8]·$G1_2$ complex (40 μM for G1) in the presence of different antibiotics (40 μM).

10. Anti-Interference Tests

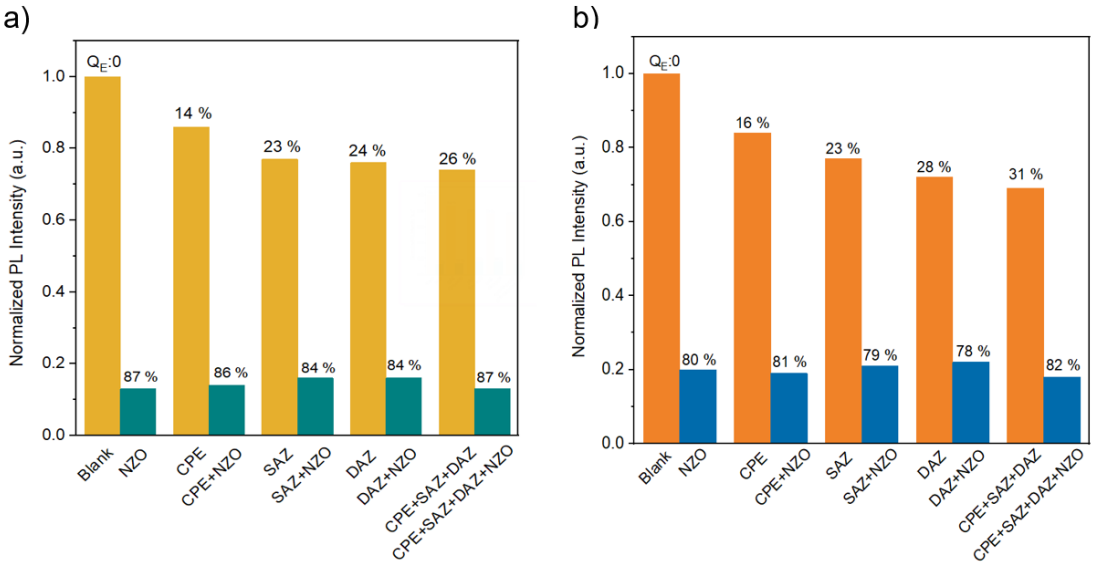

Fig. S22 Fluorescence intensities of a) WUST-1 and b) WUST-2 in the presence of separate antibiotics and the different mixtures of antibiotics (50 ppm) in solution.

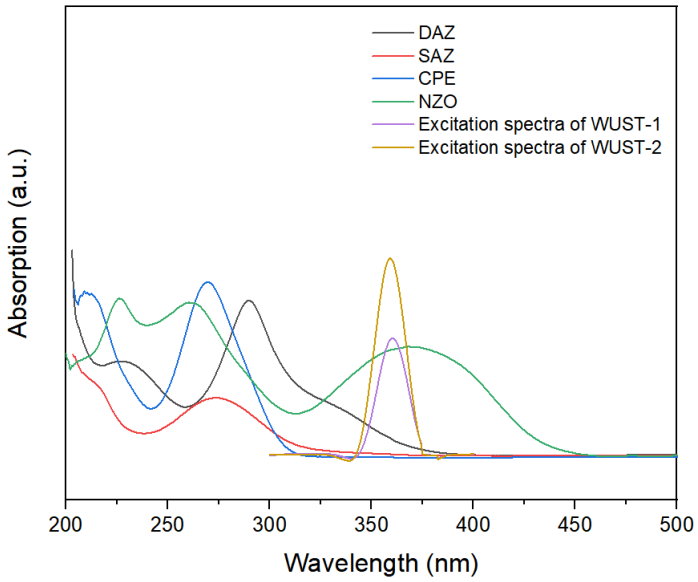

Fig. S23 Absorption spectra of different antibiotics and the excitation spectra of WUST-1 and WUST-2.

11. Stability Tests After Sensing

The crystals of WUST-1/WUST-2 (80.0 mg) were dispersed in 20 mL NZO aqueous solution (50 ppm) with ultrasonic dispersion for 1 minutes. The solution was allowed to stand at room temperature for ~10 minutes and then dried at 50 ℃ in vacuum after filtration.

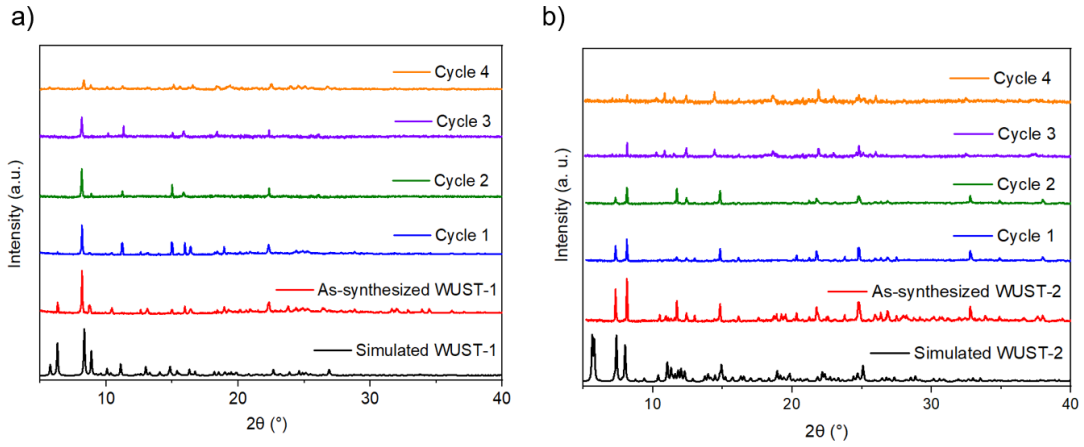

Fig. S24 PXRD patterns of a) WUST-1 b) WUST-2 after each sensing cycle for NZO.

References

1 Y. Kang, X. Tang, H. Yu, Z. Cai, Z. Huang, D. Wang, J. F. Xu and X. Zhang, *Chem. Sci.*, 2017, **8**, 8357.

2 G. M. Sheldrick, *Acta Crystallogr.*, 2008, A**64**, 112.

3 O. V. Dolomanov, L. J. Bourhis, R. J. Gildea, J. A. K. Howard and H. Puschmann, *J. Appl. Crystallogr*., 2009, **42**, 339.

4 Z. Cong, Z. Song, Y. Ma, M. Zhu, Y. Zhang, S. Wu and E. Gao, *Chem. Asian J*., 2021, **16**, 1773.

5 J. Li, T. J. Chen, S. Han and L. F. Song, *J. Solid State Chem.*, 2019, **277**,107.

6 Z. Lei, L. Hu and Z. H. Yu, *Inorg. Chem. Front*., 2021, **8**, 1290.

7 Q. Chu, B. Zhang, H. Zhou, B. Li, L. Hou and Y. Y. Wang, *Inorg. Chem*., 2020, **59**, 2853.

8 J. D. An, T. T. Wang, Y. F. Shi, X. X. Wu, Y. Y. Liu, J. Z. Huo and B. Ding, *J. Mol. Struct*., 2020, **1216**, 128328.

9 Z. H. Nie, L. Lu, M. Zheng, Z. Liao, G. Ye, A. Singh and A. Kumar, *J. Mol. Struct.*, 2021, **1245**, 131264.

10 J. L. Gu, X. W. Tao, Q. Q. Tu, A. L. Cheng and E. Q. Gao, *J. Solid State Chem.,* 2020, **286**, 121318.

11 Z. W. Zhai, S. H. Yang, M. Cao, L. K. Li, C. X. Du and S. Q. Zang, *Cryst. Growth Des*., 2018, **18**, 7173.